Chemistry & Biology, Vol. 12, 1007–1014, September, 2005, ©2005 Elsevier Ltd All rights reserved. DOI 10.1016/j.chembiol.2005.06.016

Structure-Based Discovery of a Boronic Acid Bioisostere of Combretastatin A-4

Yali Kong,[1] Jolanta Grembecka,[2] Michael C. Edler,[3] Ernest Hamel,[3] Susan L. Mooberry,[4] Michal Sabat,[1] Jayson Rieger,[1] and Milton L. Brown[1,*]

[1]Department of Chemistry
University of Virginia
Charlottesville, Virginia 22904

[2]Molecular Physiology and Biological Physics
University of Virginia
Charlottesville, Virginia 22908

[3]Screening Technologies Branch
Developmental Therapeutics Program
Division of Cancer Treatment and Diagnosis
National Cancer Institute at Frederick
National Institutes of Health
Frederick, Maryland 21702

[4]Department of Physiology and Medicine
Southwest Foundation for Biomedical Research
San Antonio, Texas 78245

Summary

Targeting the microtubule system represents an attractive strategy for the development of anticancer agents. In this study, we report a class of combretastatin A-4 (CA-4) analogs derivatized with a boronic acid moiety replacing the hydroxyl group on the C-ring of CA-4. Docking studies of the X-ray structures of our arylboronic analogs onto an X-ray structure of the α,β-tubulin heterodimer suggested that *cis*-6 was a potent inhibitor of the colchicine binding. The model indicated that there would be strong hydrogen bonding between the boronic acid moiety and Thr-179 and Val-181 of α-tubulin. We demonstrate that the *cis*-6 boronic acid bioisostere of CA-4: (1) inhibits tubulin assembly, (2) competitively displaces colchicine, and (3) is a low-nanomolar inhibitor of human cancer cell lines. We present this isostere as a class of potent analogs of CA-4.

Introduction

Tubulin is a heterodimeric protein consisting of 50 kDa α and β subunits. Because of its key role in cellular division, targeting the microtubule system of eukaryotic cells represents an attractive strategy for the development of anticancer agents. Several research studies have elucidated at least three distinct binding regions on microtubules for antimitotic agents, consisting of the taxane, vinca alkaloid, and colchicine binding sites. Both paclitaxel, a microtubule stabilizer targeting the taxane binding site, and vincristine, a microtubule destabilizer, have been successfully used in the clinic for the treatment of various cancers in human patients. Although paclitaxel is widely used in the treatment of breast cancer, it suffers from unexpected side effects, difficulty in dosing, and lack of efficacy against multidrug-resistant cancer cell lines.

The development of anticancer compounds that target the colchicine binding site has been an area of major interest. Combretastatin A-4 (CA-4), one of the most potent antimitotic agents from the combretastatin family, is a simple natural product isolated by Pettit and coworkers from a bush willow tree (*Combretum caffrum*) in South Africa [1]. CA-4 exhibits potent inhibition of tubulin polymerization through binding to the colchicine binding site.

The cytotoxic effects of CA-4 against a variety of human cancer cell lines and its activity in animal xenograft models have been reported. CA-4 was evaluated as an experimental therapeutic in humans, but poor water solubility unfortunately hindered its development as a drug. However, combretastatin A-4 phophate (CA-4P), a water-soluble disodium phosphate prodrug of CA-4, is currently in phase I/II clinical trials, with very impressive early results. Because of the clinical potential of CA-4P, a sizeable number of CA-4 analogs have been synthesized (Figure 1A) [2–5]. Several ligand based [6–8] and one structure based [9] model have been established to elucidate important SAR for the colchicine binding site. We report here a structure-based design for inhibitors of the colchicine binding site (Figure 1B).

Boronic acid inhibitors are of considerable interest in drug development, and it is well known that some boronic acid compounds are potent inhibitors of serine proteases [10]. Recently, bortezomib (VELCADE), a modified dipeptidyl boronic acid, entered phase I/II clinical trials [11, 12], and it has now received fast-track approval by the Food and Drug Administration as a treatment for multiple myeloma.

In this study, we adapted a designed methodology, using boronic acid to mimic the OH group on the C-ring of the CA-4 scaffold (Figure 1B), in an effort to provide an example of the usefulness of this group as an isostere for an aromatic hydroxyl group. Structure-based modeling was used to evaluate potential interactions of the boronic acid group with the α, β-tubulin heterodimer and to help in understanding any differences in molecular volume between CA-4 and the potential boronic acid isosteres. We also chose the boronic acid functional group in an effort to improve the water solubility of CA-4 without resorting to a prodrug strategy.

We synthesized both the *cis* and *trans* of the boronic acid isostere of CA-4. We also obtained a single crystal structure of each isomer to use as a starting geometry in our modeling studies. We then investigated their interaction with the colchicine binding site of tubulin by evaluating inhibition of [^{3}H] colchicine binding to tubulin, disruption of tubulin assembly, and effects on cancer cell growth and morphology.

Results and Discussion

The results of our modeling studies suggest that 3′-substituted boronic acids of CA-4 will mimic the 3′-OH

*Correspondence: mlb2v@virginia.edu

Figure 1. Structures of Antimicrotubule Drugs

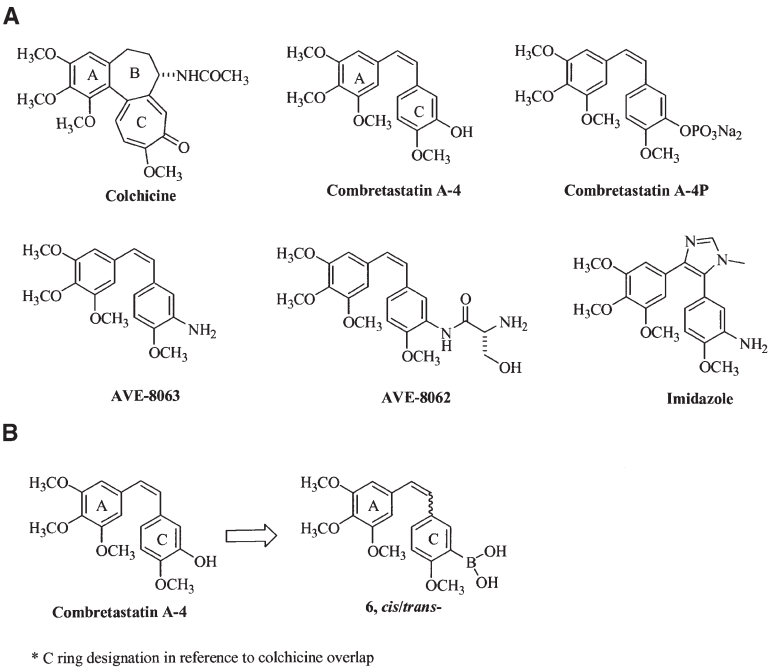

phenyl of CA-4 very well. Molecular volume calculations reveal that addition of the boronic acid appeared to add a molecular volume of 16 Å^3 (approximately the size of a water molecule) in the C-ring binding region of the analog. As our docking model predicted, we found that *cis*-**6** was a potent inhibitor of the binding of colchicine to tubulin, although it was not as strong an inhibitor as CA-4. In contrast, *cis*-**6** was more potent than CA-4 in inhibiting tubulin polymerization. Concordant with these biochemical findings, *cis*-**6** disrupted the microtubule network within the cell cytoplasm of A-10 cells. In terms of cytotoxicity, *cis*-**6** was somewhat more active than CA-4 against MCF-7 human breast cancer cells, while CA-4 was more active against the A-10 cell line. NCI cancer cell panels showed that the *cis*-boronic acid of CA-4 was also extremely potent against a wide range of human cancer cell lines. The effects of these agents on cell proliferation were stereospecific (generally, *cis*-**6** >> *trans*-**6**), as was the case in the biochemical assays.

The rare use of boron-containing isosteres in drug optimization studies is puzzling. The physical properties of boronic acids appear to make this group applicable to drug discovery. The pKa of boronic acid is approximately 9–10, so it remains largely protonated under physiological pH conditions. It has been suggested that hydrogen bonds, as well as boron-nitrogen bonds [13], can be formed, and thus boronic acid could potentially provide a functional group that enhances the interactions between a ligand and its protein receptor.

Solubility measurements for *cis*-**6** and CA-4 demonstrated that these two compounds have comparable solubility data at pH 7.4 and distilled water. The *cis*-**6** compound was, however, almost 2-fold more soluble than CA-4 at pH 2. This suggest that our compound *cis*-**6** will be stable and more soluble with oral delivery (see Supplemental Data for details).

Boron-containing compounds are usually air-stable and no special handling is needed when testing them. Moreover, there has been no reported toxicity specially associated with boronic acid isosteres, and recently VELCADE has been approved for human use in multiple myeloma. VELCADE does undergo deboronation to form 2-deboronated analogs (major metabolite), which undergo hydroxylation to several inactive metabolites [14].

CA-4P (a water-soluble prodrug of CA-4) is dephosphorylated in vivo to generate CA-4, and has a short plasma half-life [15]. CA-4P is not active at inhibiting tubulin polymerization or [^{3}H] colchicine displacement. We anticipate that hydrolysis would not occur with our boronic acid compound, because the aryl carbon-boron bond is not known to be subject to hydrolysis. The expected potential increase in hydrogen bonding of *cis*-**6** to tubulin was an additional factor in our decision to synthesize and evaluate this compound. Finally, the prospect of using *cis*-**6** after tumor debulking in conjunction with boron neutron capture therapy for treatment of residual disease is a possibility.

Chemistry

The strategy used to synthesize the *cis*-**6** and *trans*-**6** analogs is outlined in Figure 2. Briefly, 3,4,5-trimethoxybenzaldehyde **1** was reduced by $NaBH_4$ in methanol to give the alcohol **2** in 94% yield [16]. Compound **2** was treated with phosphorus tribromide to yield the bromide **3**. Reaction of **3** with triphenylphosphine gave the phosphonium salt **4** in quantitative yield. This was followed by a Wittig coupling of the phosphonium salt **4** with 3-bromo-4-methoxybenzaldehyde in the presence of NaHMDS/THF at –78°C, and resulted in a mixture of stilbenes (in a 2:1 *cis*/*trans* ratio). The *cis*/*trans* mixture

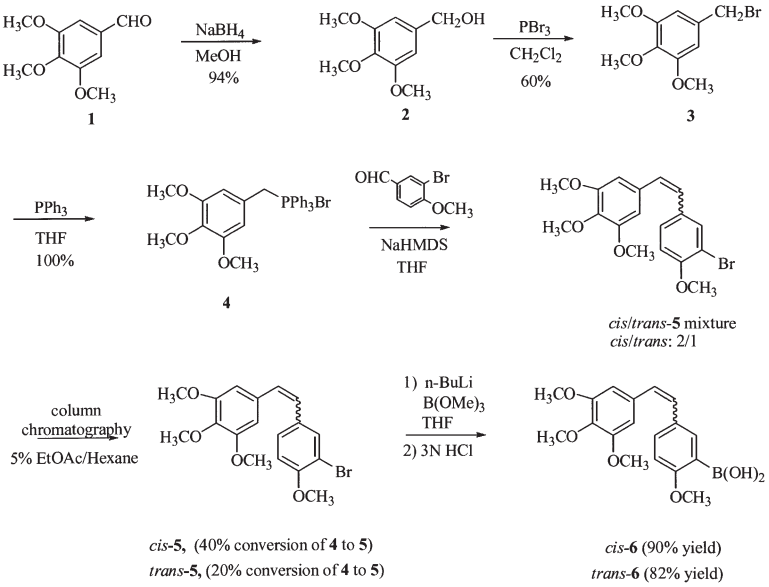

Figure 2. Synthesis of Boronic Acid Compounds *cis*-6 and *trans*-6

was purified and isomers separated by flash column chromatography in 5% ethyl acetate/hexanes (Hex). Conversion of the separated *cis* and *trans* isomers to final products *cis*-6 and *trans*-6 boronic acids was accomplished by treating *cis*-5 and *trans*-5 independently with trimethylboronate and n-butyllithium at –78°C.

X-Ray Crystal Structure

To obtain a good starting geometry for our structure based approach, we obtained single crystal X-ray structures of *cis*-6 and *trans*-6 (Figures 3A and 3B). Colorless needle crystals of *cis*-6 and *trans*-6 were obtained by recrystallization from Hex/ethyl acetate. Measurements were carried out using MoKα radiation on a Bruker SMART APEX CCD diffractometer and an Oxford Cryosystems 700 low-temperature device, and SHELXTL software was used for the structure determination.

Molecular Modeling

Surface Volume

The surface volume contour of colchicine, *cis*-6, CA-4, and water were calculated on a Silicon Graphics Octane II using SYBYL 6.8 (Tripos Inc., St. Louis, MO). The VIEW option, CONTOUR SURFACES, was used to create a VOLUME CONTOUR using default settings. The contour maps in Figure 3C represent surface volumes (at a 50.0 contour level) of the crystal structures of colchicine (extracted from the 1SA0), *cis*-6 (X-ray structure conformation), and water (SYBYL 6.8 fragment library). A low-energy structure of CA-4 was obtained by modifying the *cis*-6 X-ray structure at the 3′-position within the build/edit mode of SYBYL. Energy minimization of the representative CA-4 was accomplished by using a conjugate gradient approach with a 0.05 kcal energy cutoff. Optimization was completed in less than the 1000 iterations, defined within the COMPUTE ENERGY MODULE in SYBYL.

Docking

Recently, the X-ray structure of tubulin in complex with a colchicine analog, *N*-deacetyl-N-(2-mercaptoacetyl)-colchicines(DAMA-colchicine), was reported [17]. This structure was used to evaluate possible binding modes

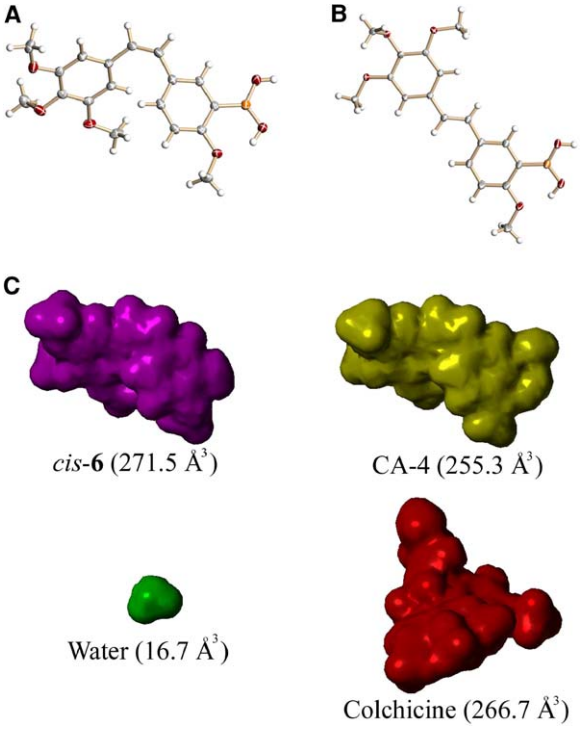

Figure 3. Crystal Structures and Surface Volumes

(A) X-ray crystal structure of *cis*-6.

(B) X-ray crystal structure of *trans*-6.

(C) Surface volume representation of *cis*-6, CA-4, water, and colchicine.

of *cis*-**6** and CA-4 to the α, β-tubulin heterodimer. Using LigandFit (Accelerys) [18], we extracted DAMA-colchicine and redocked it into the originating X-ray structure of tubulin de novo (rms = 1.1 Å between the best scored conformer resulting from docking and the binding mode from the X-ray structure of its complex with the protein) as a docking calibration.

We next identified a potential binding mode of CA-4 with tubulin using the same methodology in LigandFit and compared it to the interactions of the original DAMA-colchicine bound within the tubulin crystal structure. LigandFit, Consensus Score [18], and visual inspection were used to evaluate the proposed interactions. From this analysis, a top-scored conformer of CA-4, which was selected as the most probable binding mode, was generated.

In Figure 4, we present a representation of the results of our docking studies. Figure 4A shows the comparison of the proposed binding mode of CA-4 (red) and DAMA-colchicine (blue) originating from the X-ray structure of the complex with tubulin. The binding site is located between β and α subunits of tubulin, with the ligand molecule mostly buried in the β subunit. The binding modes of these two tubulin polymerization inhibitors are very similar. Both trimethoxy and phenyl rings in the calculated binding mode of CA-4 adopt a very similar orientation to that of the corresponding rings (A and C) in DAMA-colchicine of the crystal structure. The alkene linkage between the two rings in CA-4 corresponds to the position of the B-ring of DAMA-colchicine. Moreover, the methoxy substituent of the C ring of CA-4 is positioned in close proximity to the corresponding group of DAMA-colchicine. Furthermore, the position of the hydroxyl group of CA-4 closely resembles the position of the carbonyl oxygen of colchicine, and the latter is involved in a hydrogen bond with the backbone amide of Val 181 on the α subunit. Our model shows that a similar hydrogen bond can be formed by the hydroxyl group of CA-4. In addition, CA-4 hydroxyl group should be involved in the hydrogen bond with the carbonyl group of Thr 179 of α-tubulin. However, due to the geometry of this bond (distance about 3.9 Å), this interaction might be weaker than a normal hydrogen bond. On the other hand, colchicine cannot be involved in this interaction, as the hydrogen bond donor is required to be present in the ligand molecule. This observation is consistent with the slightly higher potency in the inhibition of tubulin polymerization observed for CA-4 (IC_{50} = 2.2 μM) as compared with colchicine (IC_{50} = 3.2 μM) [9].

The docking of *cis*-**6** by LigandFit resulted in 17 clusters with relatively small differences in the docking score values between the representatives. One of these conformers was the best scored when applying the Consensus Score (which includes Dock_Score, PLP, JAIN, PMF, and LUDI scoring functions [see Supplemental Data for details) [18]. Therefore, based both on the visual inspection and on the Consensus Scoring results, a single representative conformer was selected as the most probable binding mode of *cis*-**6** to tubulin (Figure 4B). In general, the calculated binding mode of *cis*-**6** is similar to the one described above for CA-4. However, due to the replacement of the hydroxyl group of CA-4 by a larger boronic group in *cis*-**6**, the position of the latter ligand is slightly shifted in the tubulin binding site toward the β subunit to accommodate the slightly larger boronic group (Figure 4B). Molecular vol-

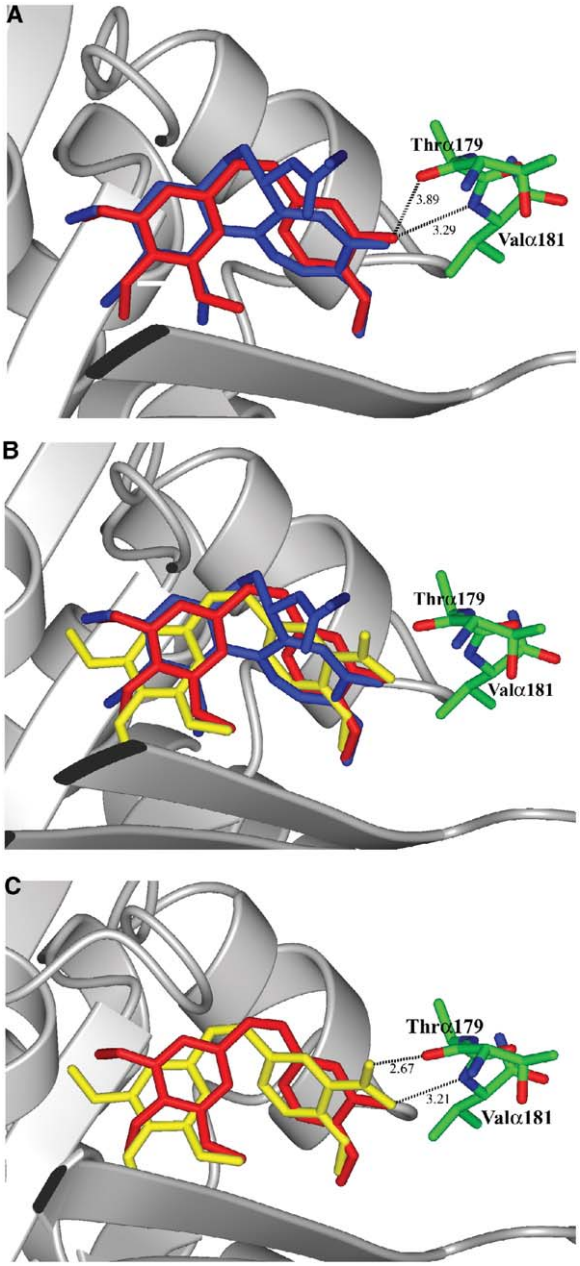

Figure 4. Binding Models of Colchicine, CA-4, and *cis*-**6**

(A) Proposed binding mode of CA-4 to tubulin. Protein originates from the X-ray structure of its complex with DAMA-colchicine (encoded as 1SA0 in PDB). DAMA-colchicine is presented in blue, CA-4 in red. β-Tubulin is shown in a ribbon representation in (A)–(C), and the residues of α-tubulin involved in the interactions with CA-4 are shown as capped sticks.

(B) Comparison of the proposed binding modes of CA-4 (red) and *cis*-**6** (yellow) to tubulin with DAMA-colchicine binding mode (blue) originating from the X-ray structure of its complex with tubulin (1SA0).

(C) Comparison of the proposed binding modes of *cis*-**6** (yellow) and CA-4 (red) to tubulin.

Table 1. Inhibition of Tubulin Polymerization, Growth of MCF-7 Human Breast Carcinoma Cells, the Binding of [^{3}H] Colchicine to Tubulin, and EC_{50} for Loss of Microtubules in A-10 Cells

Compound	Tubulin[a] IC_{50} ± SD (μM)	MCF-7[b] IC_{50} ± SD (nM)	[^{3}H] Colchicine Binding[c] (% ± SD) 5 μM	50 μM	A-10 EC_{50} (μM)[d]
cis-**6**	1.5 ± 0.2	17 ± 5	79 ± 1.7	99 ± 2.1	0.058
trans-**6**	7.8 ± 1.4	470 ± 140	13 ± 6.5	51 ± 8.1	>15
CA-4	2.0 ± 0.1	32 ± 21	99 ± 2.0	N/D	<0.025

N/D, no data.
[a] Inhibition of tubulin polymerization. Tubulin was at 10 μM.
[b] Inhibition of growth of MCF-7 human breast carcinoma cells.
[c] Inhibition of colchicine binding. Compounds *cis*-**6** and *trans*-**6** were tested at 5 and 50 μM. The tubulin concentration was 1 μM, and [^{3}H] colchicine concentration was 5 μM. All experiments were performed in triplicate with reported standard deviation (SD).
[d] The percentage of cellular microtubule loss was estimated visually over a range of concentrations. Dose-response curves were generated and EC_{50} values calculated. The values represent the results of two independent experiments.

ume studies (Figure 3C) reveal that the addition of a $-B(OH)_2$ adds approximately the molecular volume of H_2O (16 Å^3). This would make the total molecular volume of *cis*-**6** slightly larger than that of colchicine (266.7 versus 271.5 Å^3).

Our docking studies also suggest that one of the hydroxyl groups of the boronic acid is placed in a very similar position to the hydroxyl group of CA-4, and it establishes a hydrogen bond with the backbone amide of Val 181 of α-tubulin. The second hydroxyl of boronic acid in *cis*-**6** forms a hydrogen bond with the backbone carbonyl of Thr 179 of α-tubulin. The geometry for this interaction is better than that for CA-4, as the hydroxyl of the boronate in *cis*-**6** can approach closer to Thr 179 (Figure 4C). This is consistent with the slightly higher potency of *cis*-**6** for the inhibition of tubulin polymerization (IC_{50} = 1.5 μM) and the growth of MCF-7 human breast carcinoma cells (IC_{50} = 17 nM) as compared with CA-4.

Biological Data

The boronic acid analogs *cis*-**6** and *trans*-**6** were evaluated for their ability to bind to the colchicine site by inhibition of the binding of [^{3}H] colchicine. The *cis*-boronic acid **6** was slightly less inhibitory than CA-4 when evaluated at 5 and 50 μM (Table 1). However, *cis*-**6** was slightly more active as an inhibitor of tubulin polymerization (Table 1) compared with CA-4. These results demonstrate quite clearly that the *cis*-boronic acid **6** is a viable bioisostere of CA-4.

Comparison of activities of *cis*-**6** and *trans*-**6** as inhibitors of tubulin polymerization, colchicine binding, and MCF-7 cell proliferation all confirm the high selective preference for the *cis* conformation over the *trans*. These results agree with extensive literature data demonstrating the increased activity of numerous *cis* as compared with *trans* analogs of CA-4 [19].

To evaluate the effects of our isostere *cis*-**6** on intracellular microtubules, indirect immunofluorescence was used to visualize the effects of these analogs on microtubules of A-10 cells. In the control (Figure 5A), the microtubule network and nuclei are clearly visible. When the cells were treated with CA-4 (Figure 5B), the network of microtubules was completely lost, but the nuclei were still visible. However, in the cells treated with *cis*-**6** (Figure 5C), a complete loss of the microtubule network occurred, and the cell nuclei were less distinct. The corresponding EC_{50} value for each compound is shown in Table 1. For *cis*-**6**, an EC_{50} of 0.058 μM was found as a concentration at which 50% of the intracellular microtubule network of A-10 cells was disrupted. These data provide additional evidence, besides the cytotoxic results presented above and below, that boronic acid isosteres of CA-4 can easily penetrate the cell membrane in the low- to mid-nanomolar range.

The antiproliferative profile of the boronic acid CA-4 mimetics, *cis*-**6** and *trans*-**6**, were evaluated at the National Cancer Institute (NCI) against 53 human cancer cell lines. The results are shown in Table 2. Compound *cis*-**6** was extremely active toward 43 out of 53 human cancers, with GI_{50} values below 10 nM. The *trans*-**6** isomer was found to be significantly less active in every line examined except the U251 central nervous system cancer cell line. This is consistent with all of our previously presented results.

Significance

In this study, we designed boronic acid mimetics of the phenol of CA-4. The addition of boronic acid adds approximately the surface volume of the water molecule. Docking studies suggested that the combretastatin boronic acid *cis*-6 would bind to the colchicine binding site on β-tubulin as well as to amino acids on α-tubulin. We confirmed that the *cis*-6 analog was able to inhibit [^{3}H] colchicine binding to β-tubulin with a 79% inhibition at 5 μM (in 1:1 ratio with [^{3}H] colchicine). Compound *cis*-6 also inhibited tubulin polymerization with an IC_{50} of 1.5 ± 0.2 μM. Indirect immunofluorescence studies revealed that the *cis*-6 analog could penetrate the cell membrane and inhibit intracellular microtubules of A-10 cells with an EC_{50} value of 0.058 μM. Treatment of 53 human cancer cell lines with the *cis*-6 compound resulted in the growth inhibition of 43 cell lines at GI_{50} values below 10 nM. Altogether, our results demonstrate that arylboronic acids provide a viable biomimetic of phenol groups, and this isostere represents a new class of potent analogs of CA-4.

Experimental Procedures

Chemistry: General Methods

NMR spectra were recorded using a Varian-300 spectrometer for ^{1}H (300 MHz) and ^{13}C (75 MHz). Chemical shifts (δ) are given in ppm downfield from tetramethylsilane as internal standard, and coupling

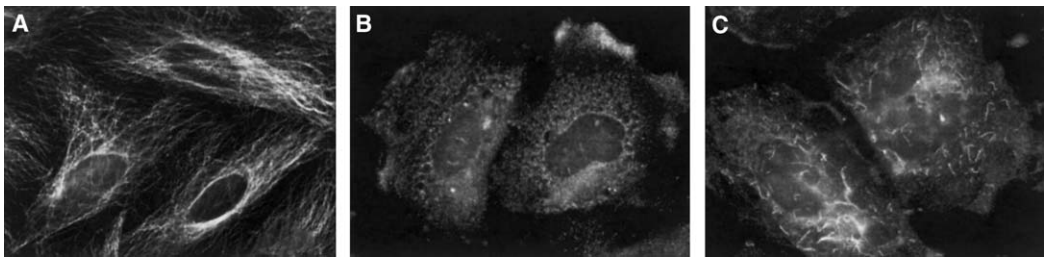

Figure 5. Effects of CA-4 and *cis*-**6** on Interphase Microtubules in A-10 Cells
(A) Vehicle control.
(B) 50 nM CA-4.
(C) 100 nM Compound *cis*-**6**.

constants (J values) are in hertz. Mass spectra data were collected on a Finnigan MAT LC-Q mass spectrometer system using electrospray ionization (ESI). Elemental analyses were performed by Atlantic Microlabs. Melting points were obtained using an electrothermal digital melting point apparatus and are uncorrected. All purifications by flash chromatography were performed using Geduran silica gel 60, 35–75 μm (VWR Scientific, West Chester, PA). All solvents used were purified by pressure filtration through activated alumina. Reactions were run at ambient temperature and under a nitrogen atmosphere, unless otherwise noted, and were monitored by TLC using Merck 60 F_{254} silica gel aluminium sheets (20 × 20 cm).

(3,4,5-Trimethoxyphenyl)methanol (2)

Sodium borohydride (1.06 g, 28.0 mmol) was added to a solution of 3,4,5-trimethoxybenzaldehyde (5.0 g, 25.5 mmol) in absolute methanol (50 ml) and stirred for 30 min. After completion of the reaction, water (15 ml) was added, and the solution was extracted with ethyl acetate (EtOAc) (3 × 30 ml). The combined extracts were washed with brine (30 ml) and dried over sodium sulfate. Rotary evaporation afforded alcohol **2** as a clear oil (4.73 g, 94%): ^{1}H NMR ($CDCl_3$, 300 MHz) δ 6.47 (s, 2H), 4.48 (s, 2H), 3.72 (s, 9H), 3.24 (s, 1H).

5-(Bromomethyl)-1,2,3-trimethoxybenzene (3)

The alcohol **2** (4.7 g, 23.7 mmol) was dissolved in dry CH_2Cl_2 (40 ml) and cooled to 0°C. Phosphorus tribromide (2.25 ml, 23.7 mmol) was added dropwise, and the reaction mixture was warmed to room temperature and stirred overnight; 5% $NaHCO_3$ was added, and the CH_2Cl_2 layer was separated and dried over sodium sulfate. The CH_2Cl_2 layer was filtered, and concentrated by rotary evaporation, and the residue was purified by flash column over silica using 5% EtOAc/Hex to give a white solid **3** (3.7 g, 60%): ^{1}H NMR ($CDCl_3$, 300 MHz) δ 6.62 (s, 2H), 4.47 (s, 2H), 3.87 (s, 6H), 3.85 (s, 3H).

3,4,5-Trimethoxybenzyltriphenylphosphonium bromide (4)

Triphenylphosphine (4.1 g, 15.6 mmol) was added to a solution of **3** (3.1 g, 12.0 mmol) in dry THF (30 ml). The mixture was refluxed with stirring for 6 hr. The resulting white solid was filtered and washed with ether/Hex to afford the product **4** in quantitative yield: ^{1}H NMR ($CDCl_3$, 300 MHz) δ 7.78 (s, 15H), 6.23 (s, 2H), 5.05 (d, 2H, J = 15 Hz), 3.59 (s, 3H). 3.36 (d, 6H, J = 15 Hz).

5-[(Z)-2-(3-Bromo-4-methoxyphenyl)vinyl]-1,2,3-trimethoxybenzene (cis-5)

Phosphonium bromide **4** (1.22 g, 2.33 mmol) was suspended in dry THF and cooled to –78°C. Sodium bis(trimethylsilyl)amide (2.56 ml, 2.56 mmol, 1.0 M in THF) was added slowly with stirring. The mixture was stirred at –78°C for 3 hr, and 3-bromo-4-methoxybenzaldehyde (0.56 g, 2.56 mmol) in 5 ml THF was added dropwise. The reaction temperature was maintained at –78°C for another hour, and the mixture was warmed to room temperature. The reaction mixture was stirred for 4.5 hr until the red solution became pale yellow. The yellow solution was poured into saturated NH_4Cl (20 ml) and extracted with EtOAc. The extracts were combined, washed with brine, and dried over Na_2SO_4. The organic layer was filtered and rotary concentrated to give the crude mixture of *cis*/*trans* stilbene **5**. Flash column chromatography using 5% EtOAc/Hex eluted the *cis*-stilbene **5** (R_f = 0.41, Hex/EtOAc = 3/1) as a white solid (354.3 mg, 40%): mp 100°C–102°C. ^{1}H NMR ($CDCl_3$, 300 MHz) δ 7.56 (s, 1H), 7.20 (d, 1H, J = 8.4 Hz), 6.73 (d, 1H, J = 8.7 Hz), 6.51 (s, 2H). 6.46 (d, 1H, J = 12.3 Hz), 6.41 (d, 1H, J = 12.3 Hz), 3.88 (s, 3H), 3.85 (s, 3H), 3.71 (s, 6H); ^{13}C NMR (75.5 MHz) δ 154.8, 152.9, 137.3, 133.6, 132.2, 131.0, 129.8, 129.3, 127.8, 111.4, 111.0, 105.9, 60.8, 56.1, 55.9; ESI *m/z* 380 $(M + H)^+$.

5-[(E)-2-(3-Bromo-4-methoxyphenyl)vinyl]-1,2,3-trimethoxybenzene (trans-5)

Flash column as described above yielded stilbene *trans*-**5** (R_f = 0.31, Hex/EtOAc = 3/1) as a pale yellow solid (180.0 mg, 20%): mp 150°C–152°C. ^{1}H NMR ($CDCl_3$, 300 MHz) δ 7.75 (d, 1H, J = 2.1), 7.40 (dd, 1H, J = 2.1, 2.1 Hz), 6.91 (s, 2H), 6.89 (s, 1H). 6.72 (s, 2H), 3.92 (s, 9H), 3.85 (s, 3H); ^{13}C NMR (75.5 MHz) δ 155.3, 153.4, 137.8, 132.9, 131.5, 130.8, 127.8, 126.8, 126.2, 112.0, 111.9, 103.4, 61.0, 56.3, 56.1; ESI *m/z* 380 $(M + H)^+$.

2-Methoxy-5-[(Z)-2-(3,4,5-trimethoxyphenyl)vinyl]boronic Acid (cis-6)

Cis-**5** (1.35 g, 3.56 mmol) was dissolved in dry THF (50 ml) and cooled to –78°C, and n-BuLi (3.34 ml, 5.34 mmol, 1.6 M in Hex) was added dropwise. The resulting mixture was stirred at –78°C for another 1.5 hr, followed by the dropwise addition of trimethyl borate (0.55 g, 5.34 mmol) dissolved in 5 ml THF. The mixture was warmed to room temperature and stirred overnight. The reaction was quenched with 3 N HCl (10 ml) and stirred at room temperature for 30 min, followed by washing with ether (3 × 30 ml). The combined ether layers were extracted with 1 N NaOH (2 × 20 ml), and the basic layers were reacidified with 1 N HCl to pH 4. After reacidification, the mixture was extracted with ether (2 × 30 ml), and the ether layers were combined. The combined ether layers were dried over Na_2SO_4, filtered, and concentrated to afford a pale yellow oil. Flash column chromatography using 20% EtOAc/Hex eluted the *cis*- **6** (R_f = 0.4, Hex/EtOAc = 1/2) as a sticky oil (1.10 g, 90%). Recrystallization of the oil in Hex/EtOAc resulted in white crystalline needles of *cis*-**6**: mp 109°C–110°C. ^{1}H NMR ($CDCl_3$, 300 MHz) δ 7.83 (d, 1H, J = 2.4), 7.34 (dd, 1H, J = 2.4, 2.4 Hz), 6.78 (d, 1H, J = 8.7 Hz), 6.52 (m, 4H). 5.81 (broad, 2H), 3.90 (s, 3H), 3.85 (s, 3H), 3.70 (s, 6H); ^{13}C NMR (75.5 MHz) δ 163.82, 153.13, 137.94, 137.29, 133.64, 132.99, 130.33, 129.60, 129.42, 129.34, 109.87, 106.09, 61.13, 56.11, 55.84; ESI *m/z* 345 $(M + H)^+$. Analysis calculated for $C_{18}H_{21}BO_6$: C, 62.82; H, 6.15. Found: C, 62.80, H, 6.21.

2-Methoxy-5-[(E)-2-(3,4,5-trimethoxyphenyl)vinyl]boronic acid (trans-6)

Compound *trans*-**6** was obtained in 82% yield from the *trans*-**5** following the same procedure as described above; mp 120°C–122°C. ^{1}H NMR ($CDCl_3$, 300 MHz) δ 8.03 (d, 1H, J = 2.4), 7.59 (dd, 1H, J = 2.7, 2.4 Hz), 7.00 (s, 2H), 6.94 (d, 1H, J = 8.7 Hz), 6.74 (s, 2H), 5.92 (broad, 2H), 3.96 (s, 3H), 3.92 (s, 6H), 3.88 (s, 3H); ^{13}C NMR (75.5 MHz) δ 164.32, 153.61, 136.06, 135.12, 133.52, 131.03, 130.62, 128.18, 127.57, 127.39, 110.55, 103.55, 61.18, 56.31, 55.93; ESI *m/z* 345 $(M + H)^+$. Analysis calculated for $C_{18}H_{21}BO_6$: C, 62.82; H, 6.15. Found: C, 62.74, H, 5.97.

Molecular Modeling

Docking

The X-ray structure of tubulin originating from the complex of two α, β-heterodimers with DAMA-colchicine, and the stathmin-like do-

Table 2. National Cancer Institute Cancer Cell Line GI_{50} Values

Cell Line	GI_{50} (μM)	
	cis-**6**	*trans*-**6**
Leukemia		
CCRF-CEM	<0.01	10.2
K-562	<0.01	4.1
MOLT-4	<0.01	13.8
RPMI-8226	<0.01	5.9
SR	<0.01	2.3
Non-small cell lung cancer		
A549/ATCC	<0.01	3.7
EKVX	<0.01	3.4
HOP-62	<0.01	5.6
HOP-92	<0.01	2.4
NCI-H226	9.92	12.5
NCI-H23	<0.01	3.3
NCI-H322M	<0.01	8.1
NCI-H460	<0.01	3.2
NCI-H522	<0.01	3.6
Colon cancer		
COLO 205	2.77	21.5
HCC-2998	<0.01	4.6
HCT-116	<0.01	4.2
HCT-15	4.62	27.3
KM12	<0.01	3.8
SW-620	<0.01	4.3
CNS cancer		
SF-268	0.029	12.0
SF-295	<0.01	3.5
SF-539	<0.01	3.3
SNB-19	<0.01	16.1
U251	5.17	2.5
Melanoma		
LOX IMVI	5.38	21.8
MALME-3M	0.039	13.0
M14	<0.01	3.9
SK-MEL-2	<0.01	12.1
SK-MEL-5	<0.01	2.7
UACC-257	ND	8.1
UACC-62	<0.01	2.9
Ovarian cancer		
IGROV1	<0.01	5.8
OVCAR-3	<0.01	16.7
OVCAR-4	15.80	22.9
OVCAR-5	<0.01	3.2
OVCAR-8	<0.01	3.6
SK-OV-3	5.38	9.4
Renal cancer		
786-0	<0.01	4.7
A498	<0.01	2.9
ACHN	9.27	32.0
CAKI-1	<0.01	18.2
RXF 393	<0.01	2.4
SN12C	<0.01	8.0
TK-10	<0.01	21.4
UO-31	<0.01	4.7
Prostate cancer		
PC-3	<0.01	2.4
DU-145	<0.01	2.6
Breast cancer		
MCF7	<0.01	3.2
NCI/ADR-RES	<0.01	2.3
MDA-MB-231/ATCC	<0.01	3.5
HS 578T	<0.01	2.5
MDA-MB-435	<0.01	3.1
BT-549	<0.01	3.3

main (SLD) of RB3 (encoded as 1SA0 in PDB) was applied for all docking experiments. The colchicine binding site, located between α- and β-tubulin, was used to perform docking of CA-4 and compounds *cis*-**6** and *trans*-**6**. The hydrogen atoms were added to the protein using the Insight II/Builder (Accelrys, San Diego, CA) program [20]. The protonation states of tubulin residues were selected for pH = 7.0. LigandFit [18] from Cerius^2 4.8.1 version [21], within the Accelrys suite of programs, was applied for all docking studies using the Dreiding force field [22]. The site for docking of ligands was defined based on the position of DAMA-colchicine in the tubulin crystal structure. The X-ray structure of *cis*-**6** and the model of CA-4, resulting from the replacement of the boronic group in *cis*-**6** by a hydroxyl group, were used as starting conformations for docking experiments. Flexible docking, employing Monte Carlo simulations (100,000 trials), was performed with LigandFit, using soft potential for interaction energy calculations [18]. The 100 lowest energy and diverse docking conformations were saved and clustered, using the Leader method with the rms distance threshold of 1.5 Å. The best member from each cluster was saved for further analysis. Moreover, several scoring functions, Dock_Score, PLP, JAIN, PMF, and LUDI, as implemented in Cerius^2 [21], were also applied to prioritize the docking conformation output with each ligand. Subsequently, a consensus score was calculated for each docked ligand in each conformation. Based on the scoring results and on the visual inspection of the proposed interaction modes, the best fit for each ligand was selected. The protein-ligand complexes were then placed in a 5 Å thick layer of water molecules and subjected to further refinement, using the Discover/InsightII program [23]. Optimization of protein-ligand models was performed using the CVFF force field, adding corresponding partial charges to all atoms. The polypeptide backbone atoms of tubulin remained frozen, while the protein side chains, ligand and water molecules were free during the optimization procedure. The conjugate gradient algorithm was applied for minimization, which was continued until the rms derivative was lower than 0.02 kcal/mol·Å. A twin cutoff (18.0 Å, 20.0 Å) was used to calculate the nonbonded interactions at each minimization step.

Biological Testing

[^{3}H] Colchicine Binding Assays

The binding of [^{3}H] colchicine to tubulin was measured by the DEAE-cellulose filter method, as described in detail previously [24]. The tubulin concentration was 1.0 μM (0.1 mg/ml), and the [^{3}H] colchicine concentration was 5.0 μM.

MCF-7 Cell Proliferation Assay

IC_{50} values for inhibition of cell growth were obtained by measuring the amount of total cell protein with the sulforhodamine B (SRB) assay [25]. The MCF7 cells were grown for 24 hr with and without drug. IC_{50} values were determined after an additional 48 hr.

Tubulin Polymerization

Tubulin polymerization was followed turbidimetrically at 350 nm in Beckman model DU-7400 and Du7500 spectrophotometers equipped with electronic temperature controllers, as described in detail previously [26]. The tubulin concentration was 10 μM (1.0 mg/ml).

Indirect Immunofluorescence

Drug effects on the microtubule network of A-10 cells were evaluated by indirect immunofluorescent techniques as previously described [27]. Cells were plated onto glass coverslips and treated with a range of compounds for 18 hr. The cells were fixed and microtubules visualized using a β-tubulin antibody, and nuclei were stained with 4,6-diamidino-2-phenylindole. Cells were examined with a Nikon ES800 fluorescence microscope, and images were captured with a Photometrics Cool Snap FX3 camera and compiled using Metamorph software.

NCI Human Cancer Cell Proliferation Assay

Compounds were tested against 53 human tumor cell lines at 5 concentrations in a 10-fold serial dilution. After a 48-hr incubation, an SRB protein assay was used to determine inhibition of cell growth. GI_{50} values were calculated from log dose-response curves (see [28] for additional details concerning this screen and the NCI's drug discovery and development program).

Solubility Testing

Solubility of *cis*-**6** and CA-4 were analyzed on a Shimadzu 10 ADVP system using a Waters' Atlantis dC_{18} (5 μm 4.6 × 150 mm) column with a linear gradient from 30%–60% MeOH/Water (containing 0.1% formic acid) over 15 min. A total of 3.0 mg of each *cis*-**6** and

CA-4 were suspended in the three solutions and agitated at 37°C for 24 hr. The supernatant was then removed and filtered through a 0.45 μm PTFE acrodisc filter. The concentration of the samples was analyzed using HPLC and quantified using a known standard of 100 μg/ml.

Supplemental Data

Supplemental Data, including crystal structure data for *cis*-**6** and *trans*-**6**, docking score values for different conformers of *cis*-**6** and CA-4, solubility data for *cis*-**6** and CA-4, and a more detailed analysis of the binding mode of CA-4 and its derivatives are available at http://www.chembiol.com/cgi/content/full/12/9/1007/DC1/.

Acknowledgments

We thank the National Cancer Institute's Developmental Therapeutics Program for testing, the William Randolph Hearst Foundation, and the University of Virginia, Department of Chemistry, for financial support.

Received: April 19, 2005
Revised: June 17, 2005
Accepted: June 30, 2005
Published: September 23, 2005

References

1. Pettit, G.R., Cragg, G.M., Herald, D.L., Schmidt, J.M., and Lohavanijaya, P. (1982). Isolation and structure of combretastatin. Can. J. Chem. *60*, 1374–1376.
2. Ohsumi, K., Nakagawa, R., Fukuda, Y., Hatanaka, T., Morinaga, Y., Nihei, Y., Ohishi, K., Suga, Y., Akiyama, Y., and Tsuji, T. (1998). Novel combretastatin analogues effective against murine solid tumors: design and structure-activity relationships. J. Med. Chem. *41*, 3022–3032.
3. Nihei, Y., Suzuki, M., Okano, A., Tsuji, T., Akiyama, Y., Tsuruo, T., Saito, S., Hori, K., and Sato, Y. (1999). Evaluation of antivascular and antimitotic effects of tubulin binding agents in solid tumor therapy. Jpn. J. Cancer Res. *90*, 1387–1395.
4. Pettit, G.R., Temple, C., Jr., Narayanan, V.L., Varma, R., Simpson, M.J., Boyd, M.R., Rener, G.A., and Bansal, N. (1995). Antineoplastic agents 322: synthesis of combretastatin A-4 prodrugs. Anticancer Drug Des. *10*, 299–309.
5. Wang, L., Woods, K.W., Li, Q., Barr, K.J., McCroskey, R.W., Hannick, S.M., Gherke, L., Credo, R.B., Hui, Y.H., Marsh, K., et al. (2002). Potent, orally active heterocycle-based combretastatin A-4 analogues: synthesis, structure-activity relationship, pharmacokinetics, and in vivo antitumor activity evaluation. J. Med. Chem. *45*, 1697–1711.
6. Brown, M.L., Rieger, J.M., and Macdonald, T.L. (2000). comparative molecular field analysis of colchicine inhibition and tubulin polymerization for combretastatins binding to the colchicine binding site on β-tubulin. Bioorg. Med. Chem. *8*, 1433–1441.
7. Zhang, S.X., Feng, J., Kuo, S.C., Brossi, A., Hamel, E., Tropsha, A., and Lee, K.H. (2000). Antitumor agents. 199. Three-dimensional quantitative structure-activity relationship study of the colchicine binding site ligands using comparative molecular field analysis. J. Med. Chem. *43*, 167–176.
8. Ducki, S., Mackenzie, G., Lawrence, N.J., and Snyder, J.P. (2005). Quantitative structure-activity relationship (5D-QSAR) study of combretastatin-like analogues as inhibitors of tubulin assembly. J. Med. Chem. *48*, 457–465.
9. De Martino, G., La Regina, G., Coluccia, A., Edler, M.C., Barbera, M.C., Brancale, A., Wilcox, E., Hamel, E., Artico, M., and Silvestri, R. (2004). Arylthioindoles: potent inhibitors of tubulin polymerization. J. Med. Chem. *47*, 6120–6123.
10. Kettner, C.A., and Shenvi, A.B. (1984). Inhibition of the serine proteases leukocycle elastase, pancreatic elastase, cathepsin G, and chymotrypsin by peptide boronic acids. J. Biochem. (Tokyo) *259*, 15106–15114.
11. Dy, G.K., Thomas, J.P., Wilding, G., Bruzek, L., Mandrekar, S., Erlichman, C., Albert, D., Binger, K., Pitot, H.C., Albert, S.R., et al. (2005). A phase I and pharmacologic trial of two schedules of the proteasome inhibitors, PS-341 (bortezomib, velcade), in patients with advanced cancer. Clin. Cancer Res. *11*, 3410–3416.
12. Lenz, H.J. (2003). Clinical update: proteasome inhibitors in solid tumors cancer. Cancer Treat. Rev. *29* (Suppl. 1), 41–48.
13. Tongcharoensirikul, P., Thompson, C.M., and Bridges, R.J. (2001). Boronic acid analogues as selective inhibitors of glutamate receptors and transporters. Abstracts of Papers. 222nd ACS National Meeting. Chicago, IL, August 26–30; American Chemistry Society, Washington, DC; MEDI-224.
14. Pekol, T., Daniels, J.S., Labutti, J., Parsons, I., Nix, D., Baronas, E., Hsieh, F., Gan, L.S., and Miwa, G. (2005). Human metabolism of the proteasome inhibitor bortezomib: identification of circulating metabolites. Drug Metab. Dispos. *33*, 771–777.
15. Dowlati, A., Robertson, K., Cooney, M., Petros, W.P., Stratford, M., Jesberger, J., Rafie, N., Overmoyer, B., Makkar, V., Stambler, B., et al. (2002). A phase I pharmacokinetic and translational study of the novel vascular targeting agent combretastatin A-4 phosphate on a single-dose intravenous schedule in patients with advanced cancer. Cancer Res. *62*, 3408–3416.
16. Olszewski, J.D., Marshalla, M., Sabat, M., and Sundberg, R.J. (1994). Potential photoaffinity labels for tubulin. synthesis and evaluation of diazocyclohexadienone and azide analogs of colchicine, combretastatin, and 3,4,5-trimethoxybiphenyl. J. Org. Chem. *59*, 4285–4296.
17. Ravelli, R.B.G., Gigant, B., Curmi, P.A., Jourdain, I., Lachkar, S., Sobel, A., and Knossow, M. (2004). Insight into tubulin regulation from a complex with colchicine and a stathmin-like domain. Nature *428*, 198–202.
18. Venkatachalam, C.M., Jiang, X., Oldfiels, T., and Waldman, M. (2003). LigandFit: a novel method for the shape-directed rapid docking of ligands to protein active sites. J. Mol. Graph. Model. *21*, 289–307.
19. Cushman, M., Nagarathnam, D., Gopal, D., He, H.M., Lin, C.M., and Hamel, E. (1992). Synthesis and evaluation of analogues of (Z)-1(4-methoxyphenyl)-2-(3,4,5-trimethoxyphenyl)ethane as potential cytotoxic and antimitotic agents. J. Med. Chem. *35*, 2293–2306.
20. Accelrys Inc. (2003). Insight, I.I. version 2000.2 (computer program). (http://www.accelrys.com).
21. Accelrys Inc. (2003). *Cerius*^{2} version 4.8.1 (computer program). (http://www.accelrys.com).
22. Mayo, S.L., Olafson, B.D., and Goddard, W.A., III. (1990). Dreiding: a generic force field for molecular simulations. J. Phys. Chem. *94*, 8897–8909.
23. Accelrys Inc. (2003). Discover version 2.98 (computer program). (http://www.accelrys.com).
24. Verdier-Pinard, P., Lai, J.Y., Yoo, H.D., Yu, J.R., Marquez, B., Nagle, D.G., Nambu, M., White, J.D., Falck, J.R., Gerwick, W.H., et al. (1998). Structure-activity analysis of the interaction of curacin A, the potent colchicine site antimitotic agent, with tubulin and effects of analogs on the growth of MCF-7 breast cancer cells. Mol. Pharmacol. *53*, 62–76.
25. Skehan, P., Storeng, D., Scudiero, D., Monks, A., McMahon, J., Vistica, D., Warren, J.T., Bokesch, H., and Boyd, M.R. (1990). New colorimetric cytotoxicity assay for anticancer-drug screening. J. Natl. Cancer Inst. *82*, 1107–1112.
26. Hamel, E. (2003). Evaluation of antimitotic agents by quantitative comparisons of their effects on the polymerization of purified tubulin. Cell Biochem. Biophys. *38*, 1–21.
27. Tinley, T.L., Randall-Hlubek, D.A., Leal, R.M., Jackson, E.M., Cessac, J.W., Quada, J.C., Jr., Hemscheidt, T.K., and Mooberry, S.L. (2003). Taccalonolides E and A: plant-derived steroids with microtubule-stabilizing activity. Cancer Res. *63*, 3211–3220.
28. Developmental Therapeutics Program, NCI/NIH (2005). Screening services (http://dtp.nci.nih.gov/branches/btb/ivclsp.html).